Available online at www.sciencedirect.com

ScienceDirect

Procedia CIRP 41 (2016) 1017 – 1022

www.elsevier.com/locate/procedia

48th CIRP Conference on MANUFACTURING SYSTEMS - CIRP CMS 2015

Compensating warpage of 3D printed parts using free-form deformation

Christoph Schmutzler[a,*], Alexander Zimmermann[b], Michael F. Zaeh[a]

[a]*Institute for Machine Tools and Industrial Management, Beim Glaspalast 5, 86153 Augsburg, Germany*
[b]*FORWISS University of Passau, Innstraße 43, 94032 Passau, Germany*

* Corresponding author. Tel.: +49-821-56883-47; fax: +49-821-56883-50. *E-mail address:* Christoph.Schmutzler@iwb.tum.de

Abstract

3D printing is a common technique for producing complex parts or molds in a small series scale by using ink-jet technology. The size accuracy is of great importance for the use of this technology in the manufacturing sector. However, the chemical solidification reaction of the powder with the binder during the fabrication of parts results in shrinkage. Warpage results whenever shrinkage does not occur uniformly throughout the entire part. Consequently, the size deviation is a result of the layer-wise printing process and the inhomogeneous shrinkage. A possibility to reduce these deviations is a pre-deformation of the part data, contrary to the expected defect. This is implemented by using a free-form deformation (FFD) approach. The FFD deforms the surrounding cuboid of an object in order to adapt the embedded object. Thus, an increased size accuracy is achieved by choosing suitable parameters for the FFD.
This paper describes the implementation of the FFD to compensate the significant, frequently appearing defects in the 3D printing process. The relevant defect types and typical values for the deviation are presented. Furthermore, factors of influence are identified and the deviations are described by mathematical functions. These functions are transferred to an application for the FFD. The effect of the FFD is shown for reference parts and suitable compensation parameters are presented. Finally the knowledge-based transfer to related geometries is investigated and the effect of the compensation is discussed.

Peer-review under responsibility of the scientific committee of 48th CIRP Conference on MANUFACTURING SYSTEMS - CIRP CMS 2015

Keywords: 3D Printing; Deformation; Compensation

1. Introduction

Additive manufacturing includes a multiplicity of different processes that build up parts in successive layers or units [1]. Some important advantages of these technologies are the automated production of complex part structures without specific tools directly from the CAD data [2]. As a result of the continuous development of these technologies typical applications besides the rapid prototyping have been established on the market in the sectors tooling and manufacturing [3]. Thus, for an economical use of this technology in these sectors, an improved size accuracy is required [4].

In 3D printing layers of powder are successively solidified by a selective deposition of binder with an ink-jet print head [5]. In this paper a polymer process of the company voxeljet AG is described. The material systems, called PolyPor A and PolyDens, consist of a PMMA based powder and styrol based binder. The chemical reaction of binder and powder creates a local cohesion.

2. Warpage effects caused by shrinkage

The phase change from liquid to solid upon solidification decreases the specific volume [6]. The result is a shrinkage of the printed component. Shrinkage can be easily compensated by scaling up the component, if the effect arises homogenously [6]. Warpage appears whenever the shrinkage occurs inhomogeneously across the part during the build process. The main reasons for an inhomogeneous shrinkage of the parts in the 3D printing process are the time delayed solidification of the layers as well as influences due to the part geometry and boundary effects on the surface [7]. The consequence is a change of the part shape. The objective is to compensate the resulting deviations by adapting the building data of the part. For this purpose, the effects that cause the deformations and their factors of influence must be known for a knowledge based pre-compensation.

A well-known defect in additive manufacturing is the **curling effect**. Time delayed shrinkage of the separate part layers

Peer-review under responsibility of the scientific committee of 48th CIRP Conference on MANUFACTURING SYSTEMS - CIRP CMS 2015
doi:10.1016/j.procir.2015.12.078

leads to different elongations [8]. This results in residual stresses in the part, leading to an upward bending, comparable to a bimetal [9]. In the examined process, the curling effect occurs particularly in the components' edge regions. In the interior part, tensions can relax by creeping effects due to low strength values of the material at the beginning of the solidification reaction.

A further consequence of the delayed shrinkage is **trapezoid deformation** of vertically disposed edges of the part. This effect is also caused by force transmission between the layers. Down skin surfaces contract without the interaction to adjacent layers. The delayed shrinkage of further layers on the one hand leads to an additional compression of printed layers below. On the other hand, the shrinkage of subsequently printed layers is inhibited by force transmission, thus distortion is induced.

Another significant distortion occurs, when the part has undercuts or cavities. In contrast to printed areas, loose powder is not subject to the shrinkage effect. Thus, enclosed powder causes a resistance against the contraction of the part. This results in a distortion of the part due to its geometry, called **blocked shrinkage**.

Binder evaporates partly before the chemical reaction starts. This effect is particularly strong at the surface. Thus, the solidification reaction is completed in this area faster than in the inner regions. This leads to a subsidence of side planes in massive areas of the component, referred to as **pincushion effect**.

An example of the described warpage effects is shown in Fig. 1.

3. Description of warpage and factors of influence

To develop a method for compensation, these warpage effects were investigated. Therefore, reference parts were produced and a parameter variation was done to identify factors of influence. The varied parameters were the size and orientation of the component, the material system and the amount of the dispensed binder. Moreover, the shape of the deformation was analyzed and characterized by a mathematical function. In the following explanation, a Cartesian coordinate system is used. The coordinate system refers to a horizontally oriented part and the axis system of a 3D printer. The X-axis is the horizontal direction, the Y-axis is the transverse direction and the Z-axis describes the vertical one (see Fig. 1). The description of the defects differentiates between part and position dependent effects. This determines how the component should be compensated later. A part effect only depends on the geometry of the component. However, for a position dependent effect orientation of the part in the build chamber must be considered, too.

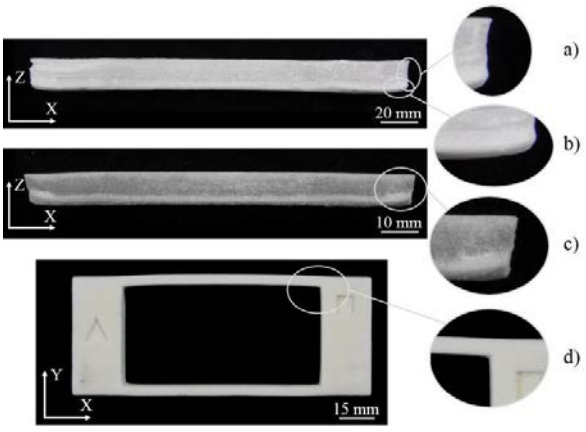

Fig. 1. Typical warpage effects in 3D printing [7]
a) pincushion effect c) trapezoid deformation
b) curling d) blocked shrinkage

The experiments were performed on a VX800 of the company voxeljet AG. As reference objects a tensile bar with the dimensions of 95 x 20 x 8 mm³ and a frame with the dimensions of 60 x 24 x 10 mm³ and a strut cross section of 2 mm were used (see Fig. 1 and 8). For the post-process the recommended standard parameters of the company voxeljet AG were employed. Subsequently, the parts were measured with the laser scanner ScanControl 2700 of the company Micro-Epsilon.

3.1. Curling

For subsequent compensation, the curling effect is, similar to the curl factor [4], described by three factors (see Fig. 2):

- d: width of the effect measured from the edge
- h_1: height of the deviation on the down skin
- h_2: height of the deviation on the upper skin

For the example of a longish, horizontally orientated component, the defect arises in Z-direction along the X-axis. The affected area in X-direction is defined by the factor d. In Z-direction the factor h determines the size of the deviation. The greatest effect occurs in this case at the down skin. With increasing thickness of the part, deviation on the top decreases. Because of this, a differentiation between upper and down skin is necessary.

The factor h_1 is used to analyze influencing values. Two different **material systems** were investigated. Using standard process parameters, PolyPor is a porous material operating at a low binder entry, thus only contact points of the powder particles are solidified. In contrast, PolyDens systems work at a high binder entry so the majority of the pores are filled with binder. The result is a more dense material, but also a higher shrinkage and warpage [10]. Thus, the deviation in PolyDens is by up to a factor of 8 higher than in PolyPor.

The binder entry is the amount of binder, which is dispensed related to the powder mass. It is adjusted by measuring the mass of one droplet and adapting the voxel size by the print resolution. Typically a binder **entry** of 10 to 15 %, related to the mass of the powder, is used. By variation of the binder entry, an almost linear increase of the defect between 10 and 20 % was detected. From 20 to 25 % binder entry, no significant change was determined and above 30 % the deformation decreases considerably. Thus, at 20 to 25 %, the deviation is about twice as large as at 10 or 30 %. This also occurs at the blocked shrinkage and the trapezoid deformation. It is assumed, that below 20 % of binder entry solidification results predominantly from incipient dissolution of the powder with subsequent evaporation of the

binder. With increasing binder entry, the amount of polymerizing binder rises. However, there is a lower shrinkage due to polymerization than due to incipient dissolution. Consequently, warpage is reduced at high binder entry.

The **angular position** of the part during production also affects the occurrence of the deformation. The example of a thin, longish component showed, that even small angle variations of 5° related to a horizontal orientation reduce the deviation by about 30 %. At a vertical orientation, the effect disappears almost completely. In explaining this context, it is assumed that shrinkage occurs stronger within a layer than in build-up direction. Thus, warpage depends on the components' cross sections and the effect is classified as position dependent effect.

Regarding the component **size**, only a slight increase of the deviation was determined for the investigated parts with a length above 80 mm. This is explained by creep effects in an interior component area and a faster solidification of the surface.

3.2. Trapezoid deformation

The trapezoid deformation is described by two factors:

- *b*: width of the deformation measured from the edge
- *h*: height of the effect measured form the down skin

The effect appears at all side surfaces of voluminous geometries perpendicular to the Z-axis. In the mathematical description of the deformation, the effect arises in X-direction defined by the parameter *b* along the Z-axis, specified by the parameter *h* (see Fig. 2). The deformation is characterized by an inclined distortion of side surfaces and a rounding of the lower part edges.

To analyze dependencies, the factor *b* and the angular deviation relating to the Z-axis determined by *h* and *b* is used. While processing the **material system** PolyDens, an increase of the deviation up to 100 % was observed. Particularly in the case of PolyDens, a strong superposition of the effect with the curling effect was determined, resulting in a large statistical spread of the measured values.

The **orientation** of the part during the fabrication has again a significant influence on the effect. The maximum deformation was identified at an angular position of about 45° for PolyPor. In this case, the deviation is approximately twice as large compared to the horizontal orientation. At vertical orientation, the effect does almost not occur at all. Thus, the deformation is also specified as a position dependent effect.

Concerning the part **size**, the progression of the deviation is declining. In this case, by doubling the component dimensions, the deviation of PolyPor rises by roughly a factor of 1.6. It is assumed, that this correlation is also caused by creeping effects.

3.3. Blocked shrinkage

To describe the blocked shrinkage, four factors are relevant:

- *h*: Height of the deviation due to shrinkage
- d_1: Beginning of the warpage measured from the edge
- d_2: Width of the transition region measured from d_1
- λ: Position of the inflection point within the interval d_2

In the mathematical description, the deviation occurs along the X-axis in Y-direction. The difference between the part shrinkage and the inhibited shrinkage caused by loose powder at the cavity in Y-direction is defined by *h*. In X-direction the deviation shows a transition region at the beginning of the cavity, see Fig. 1. The start point of this transition region is defined by d_1 and the width by d_2 (see Fig. 2). Due to the change of the curvature of the function an inflection point within the region d_2 is necessary, described by the parameter λ.

Factor *h* is used to investigate influencing parameters. The **material system** also has a strong influence. For PolyDens the deviation is about 200 % greater than for PolyPor caused by a higher shrinkage of PolyDens during solidification.

Comparing the horizontal to the vertical **orientation** of the component, an increase of the deviation of about 40 to 50 % was determined. This is the result of measuring the maximum value of the defect. Due to the layer wise fabrication, shrinkage does not appear uniformly referred to the cavity at vertical orientation. Thus, in this case the effect arises not symmetrically, is stronger in the lower region of the part due to the delayed shrinkage and decreases towards the upper region. Consequently, the average deviation is minor. For this reason the deformation is classified as a part effect for first compensation tests.

Regarding the **size** of the part the progression is declining. The reason for this is a uniform scaling of the part in all dimensions. Thus, the stiffness of the deformed area rises through the disproportionately growing resistance to bending. The factor of the growth depends on the dimensions of the part. E. g. at a cavity of 40 mm length and a strut cross section of 2 mm the deviation approximately doubles at scaling with the factor 2, but only triples by scaling with the factor 4.

3.4. Pincushion effect

The pincushion effect could be described by two factors:

- *t*: depth of the deformation due to shrinkage
- *b*: width of the transition region measured form the edge

In contrast to the previous deformations, the effect can appear in all directions. It occurs at a surface starting from the edges towards the middle of the component. Thus, the coordinate system must be adapted to the surface, at which the defect should be compensated. The value of the shrinkage perpendicular to the surface is described by *t* and the width of the transition region within the surface plane is defined by *b* (see Fig. 2).

To detect influencing factors, the parameter *t* is used. Regarding the influence of the **material** system, the effect is about 50 % stronger for PolyDens than for PolyPor. Concerning the **orientation**, the deviation roughly doubles within a layer plane compared to the build-up direction. This is due to the anisotropy of the material through the layered fabrication, whereby a lower cohesion between the layers than within a layer exists. In varying the **size**, a linear relation to the deviation was determined within statistical spread. Thus, the deformation scales with the component size. Relating to the binder **entry**, the effect is even negative at high entry values (above 25 %). This is due to the capillary transport of liquid within the powder bed. At a high

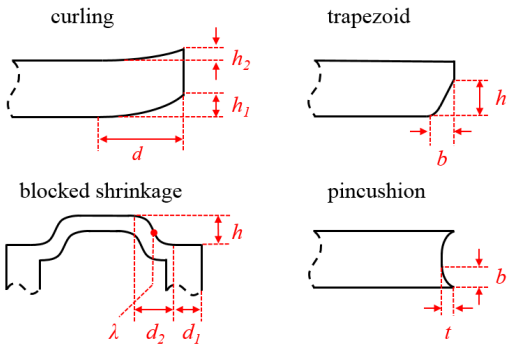

Fig. 2. Parameters to describe size deviations caused by warpage

binder entry, the pores are saturated and the binder continues to spread contrary to the deformation. Based on the high complexity of the effect with respect to the compensation of variable components, it is initially treated as a part effect.

3.5. Diagrams

The following diagrams (Fig. 3) show an excerpt of the results of the measured test objects. In this study always one parameter was varied while the other parameters were constant. The initial condition for these parameters was:

- material system: PolyPor
- binder entry 15%
- orientation: horizontal (0°)
- size: scaling factor 1

The diagrams show the value of the deformations and their standard deviation.

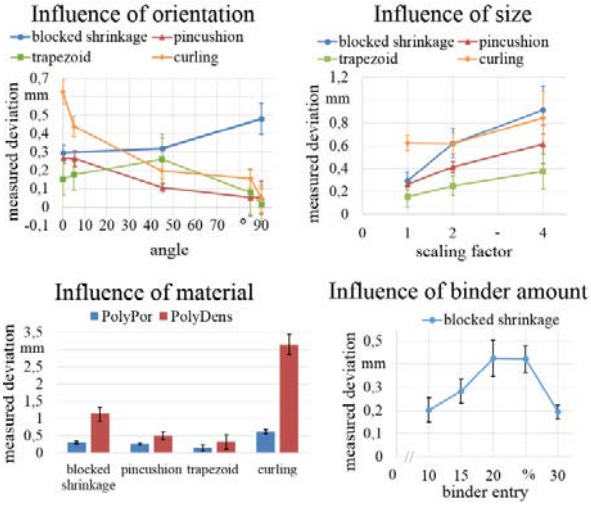

Fig. 3. Influence of the variation of orientation, size, material and binder entry

4. Free-from deformation

Free-form deformation (FFD) is a geometric technique used to model deformations of rigid objects [11]. It is based on the idea of enclosing an object within a cuboid and transforming the embedded object as the whole cuboid is deformed.

In this project trivariate B-spline functions for defining FFDs are used. A point (x, y, z) inside the definition cuboid of the FFD is transformed via the equation

$$FFD(x,y,z) = \sum_{i=0}^{n_1}\sum_{j=0}^{n_2}\sum_{k=0}^{n_3} P_{i,j,k} \cdot N_{i,p,\tau}(x) \cdot N_{j,q,\nu}(y) \cdot N_{k,r,\eta}(z), \quad (1)$$

where $N_{i,p,\tau}(x)$ is the i-th univariate B-spline function of order p with break-point sequence τ [12]. The $P_{i,j,k}$ are the so called control points of the FFD. The order describes the smoothness of the FFD in each dimension. A higher order results in smoother blending, but requires longer break-point sequences. The break-point sequence defines the flexibility of the FFD. Longer break-point sequences lead to more control points and are therefore more difficult to handle.

For every choice of definition cuboid, orders and break-point sequences, a unique set of control points exists that describes the identity-FFD, a FFD that leaves the whole cuboid unchanged. This identity-FFD is the basis for defining the deformation and pre-deformation of the part data. Some examples are shown in the next section.

5. Implementation of FFDs

In a first step we describe the relevant defect types from 3D-printed parts with FFDs. A FFD is defined by:

- the dimensions of the enclosing cuboid in three directions
- the order of spline function for each direction
- the break-point sequence for each direction
- the positions of the control points

The mathematical description of the defects utilizes primarily splines of second (linear functions) or third (quadratic function) order. For the implementation of the FFD the coordinate system is adjusted so that the Z-axis always points in the main direction of the effect. In the following examples it is shown how FFDs can be used to describe various deformations.

Since **curling** is a position dependent deformation, the Z-axis of the FFD is identical to the vertical axis of a 3D printer. It is described by the parameters d, h_1 and h_2 (see section 3.1). A spline of 3rd order with two inner break-points for the X-direction and splines of 2nd order with no inner break-points for

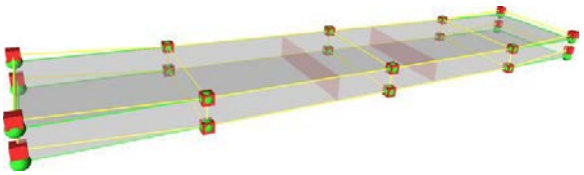

Fig. 4. Curling deformation

Fig. 5. Trapezoid deformation

the Y- and Z-direction are used. This leads to 20 control points. In Fig. 4 the parameters d = 40 mm, h_1 = 1.5 mm, h_2 = 1 mm are used to show the definition cuboid (grey box) of size 100 x 20 x 4 mm³, the inner break-point planes (red planes), the control points of the identity-FFD (green balls) and the control points of the curling deformation (red cubes).

The description of the **trapezoid deformation** uses the parameters b and h (see section 3.2) and a spline of 2nd order with two inner break-points for the X-direction, a spline of 2nd order with no inner break-points for the Y-direction and a spline of 3rd order with two inner break-points for the Z-direction. This leads to 40 control points. Fig. 5 demonstrates a definition cuboid of size 100 x 20 x 10 mm³ for the parameters b = 5 mm and h = 8 mm.

To describe the **blocked shrinkage,** the parameters d_1, d_2, λ and h are applied (see section 3.3). The mathematical description uses a spline of 3rd order with eight inner break-points for the X-direction and splines of 2nd order with no inner break-points for the Y- and Z-direction, leading to 44 control points in total. In Fig. 6 an example for the blocked shrinkage with a definition cuboid of size 100 x 20 x 4 mm³ and the parameters d_1 = 10 mm, d_2 = 20 mm, λ = 0.5 and h = 4 mm is shown.

The **pincushion effect**, described by the parameters b and t (see section 3.4), uses a 3rd order spline with two inner break-points for each direction for the FFD. This leads altogether to 125 control points. Fig. 7 illustrates a definition cuboid of size 50 x 50 x 50mm³ for the parameters b = 10 mm and t = 4 mm.

After modelling the warpage of the 3D printing process the next step is to define pre-deformations for all relevant defect types. This is accomplished by applying the negated FFD to the parts, taking into account an individual damping or enhancement factor for each defect type.

The basic operation is thereby independent from the actual defect type. The movement of the control points from the identity-FFD to the FFD describing a defect type is reversed to the opposite direction and multiplied by the appropriate factor to get the pre-deformation.

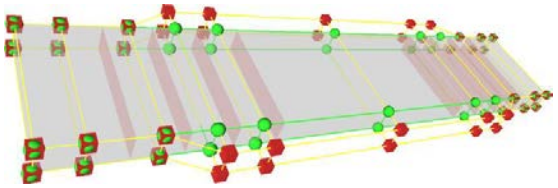

Fig. 6. Blocked shrinkage deformation

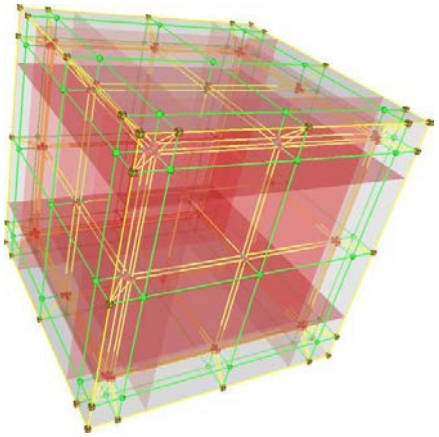

Fig. 7. Pincushion deformation

6. Compensation using FFD

For initial studies of warpage compensation the measured deformation is projected negatively onto the STL-model using the previous description of the effects for FFD. In Fig. 8 the pre-compensation is exemplarily shown for the effects curling, blocked shrinkage and trapezoid deformation.

First investigations of pre-compensation were performed on a laboratory machine called VTS128 in order to verify the effect of the compensation. Due to the higher layer time of this machine a higher amount of binder evaporates before the solidification reaction starts. This can lead to variances with respect to the values shown above (Fig. 3).

Concerning the **curling** effect the orientation as an important factor of influence was varied. By compensation the deviation was reduced at an angular position of 0° from 0.3 mm to 0.15 mm, at 5° form 0.2 mm to 0.1 mm and at 45° from 0.15 mm to less than 0.05 mm. For the angular position of 85° and 90° no effect was determined within the statistical spread.
For the **blocked shrinkage** the binder entry was examined as an influencing factor. The entry was varied from 10 to 25 % in steps of 5 %. All results showed an overcompensation of the distortion. Based on a deviation of 0.2 mm of a not compensated component at an entry of 10 % and 15 % even a degradation of the size accuracy at -0.2 to -0.3 mm was determined. At a higher entry of 20 and 25 % the compensation reduced the maximum deviation from about 0.4 mm at -0.1 to -0.2 mm.
Regarding the **trapezoid deformation**, a direct improvement was achieved by compensation. The deviation decreased from about 0.3 mm to less than 0.05 mm.

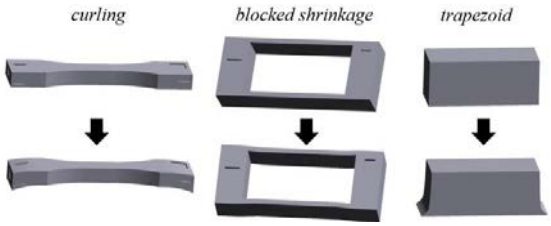

Fig. 8. Examples of pre-compensation

To examine the transferability and combinability of the results, a benchmark part was developed, see Fig. 9. The rods at position 1 and 2 are used to demonstrate the compensation of curling along the X-axis in Z-direction and blocked shrinkage along the X-axis in Y-direction. The cuboid at position 3 is used to compensate the trapezoid deformation and the pincushion effect in future investigations. The results of the study are illustrated in table 1.

Table 1. Results of the pre-compensation

position	effect	value of pre-compensation [mm]	value of deviation [mm]	
			uncompensated	compensated
1	curling	0,25	0,27	0,16
2	curling	0,25	0,22	0,10
1	blocked shrinkage	0,4	0,21	-0,37
2	blocked shrinkage	0,4	0,19	-0,38
3	trapezoid	0,3	0,67	0,40

The investigation has shown, that an improvement of the size accuracy is possible. Nevertheless, a refinement of the parameters is feasible. In the case of curling, a scaling factor is suitable, pre-compensating the deformation even stronger than it occurred. Regarding the blocked shrinkage a negated pre-deformation based on the measured values always leads to an over-compensation. This is because of the stiffening of the previously straight strut through the curved pre-compensation. Consequently, for pre-deformation it is promising to search a scaling factor less than 1 in relation to the measured values, in order to achieve better results for the compensation of this effect. For the trapezoid deformation the effect of pre-compensation is almost directly transferred to the component without using a scaling factor. In preliminary studies the effect was primarily analyzed at long, thin objects. The experiment for the benchmark part has shown that in this case an extension of the investigation concerning geometric influences is necessary.

Future investigations focus on the transfer and the refinement of the compensation onto a commercial VX800. Furthermore, the applicability of the results to similar geometries will be analyzed. On this basis, a criteria catalog should be developed to enable an experience-based pre-deformation. The acquired knowledge should be embedded into the pre-compensation software in order to identify critical component areas automatically and to propose the user appropriate parameters for the compensation.

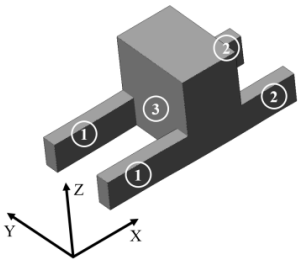

Fig. 9. Benchmark part for applying compensation

7. Conclusion

Inhomogeneous shrinkage during solidification in 3D-printing results in several forms of distortion. In this paper the four most important determined deformations are introduced and described by a mathematical function in order to develop a method for an experience-based pre-compensation of the deviation. For this purpose influencing factors on the process are relevant. Therefore, the impact of the modification of four significant parameters is shown.

To increase the size accuracy a free-form deformation approach is pursued. Based on the mathematical description a method to recreate and to compensate the distortion in the STL-data is developed for each effect. Subsequently, first results when testing the pre-compensation are presented.

The investigation revealed that an improved size accuracy can be achieved through pre-deforming of the construction data. Nevertheless, in several cases it is not sufficient to apply the measured deviation negatively to the component model. Instead, scaling factors for compensating these effects must be found in further work to ensure maximum size accuracy.

Acknowledgements

The results were developed within the research project “Intelligent Deformation Compensation for 3D-Printers” subsidized by the Bavarian Research Foundation. The authors sincerely thank the foundation and the partners for their support and the good cooperation.

References

[1] VDI 3405. Additive manufacturing processes, rapid manufacturing - Basics, definitions, processes. Düsseldorf: Beuth; 2014.
[2] Gebhardt, A. Generative Fertigungsverfahren. Additive Manufacturing und 3D-Drucken für Prototyping - Tooling - Produktion. München: Hanser; 2013.
[3] Gibson I, Rosen DW, Stucker B. Additive Manufacturing Technologies. Boston: Springer; 2010.
[4] Eschey C. Maschinenspezifische Erhöhung der Prozessfähigkeit in der additiven Fertigung. München: Utz; 2013.
[5] Kellner I. Materialsysteme für das pulverbettbasierte 3D-Drucken. München: Utz; 2013.
[6] Jacobs P. The effects of random noise shrinkage on rapid tooling accuracy. Materials & Design (2000) vol. 21, p. 127-136.
[7] Schmutzler C, Günther D, Zäh M. Minimierung der Deformationen von 3-D-gedruckten Bauteilen. Augsburger Seminar für Additive Fertigung. München: Utz; 2014.
[8] Yang H-J, Hwang P-J, Lee S-H. A study on shrinkage compensation of the SLS process by using the Taguchi method. International Journal of Machine Tools & Manufacturing (2002) vol. 42, pp. 1203-1212.
[9] Held M, Pfligersdorffer C. Correcting warpage of laser-sintered parts by means of a surface-based inverse deformation algorithm. Engineering with Computers 25 (2009) vol 4, p. 389-395.
[10] Hellmann G, Kottlorz C, Presser J, Utaloff K. Compact polymeric 3D prints of hith stability. Journal of Materials Research (2014) vol. 29 iss 17, p. 1833-1840.
[11] Sederberg T, Parry S. Free-form deformation of solid geometric models" SIGGRAPH Computer Graphics (ACM) 20 (1986) vol. 4, p. 151–160.
[12] De Boor C. A Practical Guide to Splines. Berlin: Springer; 1987.